RICE UNIVERSITY

AN EXPERIMENTAL STUDY OF SWITCHING IN A COANDA WALL

ATTACHMENT DEVICE

by

William J. Spargo

A THESIS SUBMITTED
IN PARTIAL FULFILLMENT OF THE
REQUIREMENTS FOR THE DEGREE OF

MASTER OF SCIENCE

Thesis Director's signature:

Houston, Texas

September 1969

Abstract

AN EXPERIMENTAL STUDY OF SWITCHING IN A COANDA WALL

ATTACHMENT DEVICE

by

William J. Spargo

An experimental study was conducted to determine the effect of wall angle, wall offset, and power jet pressure on the control signal required to switch the flow in a Coanda wall attachment device. A stability parameter was defined as the ratio of the power jet pressure to the change in control pressure required for switching to occur. When this ratio is a minimum, maximum stability has been attained. Data was obtained for wall angles from zero to fifty degrees; wall offsets from one-half to none inches; and power jet pressures in the range from 0.7 to 4.0 inches of mercury.

Comparisons were made between the stability parameter, the wall angle, and the wall offset to find the most stable configuration of the wall. This configuration was a wall angle of thirty degrees and a wall offset of one inch. The stability parameter remained approximately constant for different power jet pressures at each geometric configuration.

Table of Contents

Nomenclature

g - acceleration of gravity - feet per second

P_{atm} - atmospheric pressure - inches of mercury

P_{oc} - control jet stagnation pressure - inches of water gauge

P_{omg} - power jet stagnation pressure - inches of mercury gauge

P_{om} - power jet stagnation pressure corrected to standard sea level - inches of mercury gauge

$\dfrac{P_{om}}{\Delta P_{oc}}$ - stability parameter, the ratio of the power jet stagnation pressure to the change in control stagnation pressure required for switching

P_{sc_1} - control jet static pressure in the control diffuser outlet - inches of water gauge

P_{sc_2} - control jet static pressure in the control jet nozzle throat - inches of water gauge

P_{sm} - power jet static pressure in the power jet nozzle throat - inches of water gauge

T_o - power jet stagnation temperature - $^\circ F$

V - jet velocity - feet per second

Z - height above datum - feet

α - angle the wall makes with the centerline of the device - degrees

δ - wall offset measured from the near edge of the power nozzle - inches

ρ - density of air - slugs per cubic foot

Introduction

A wall attachment device is most easily understood by considering a submerged jet as shown in Figure 1. Due to the high shear at the edges of the jet, it entrains fluid from its ambient fluid. Placing a wall on one side of the jet limits entrainment on the side of the jet near the wall and thereby lowers the local pressure on that side. This pressure gradient deflects the jet toward the wall which further limits the entrainment and further reduces the local pressure of the ambient fluid on that side. Ultimately, the jet attaches to the wall trapping a recirculation bubble between the wall and the jet. Employing two walls, as shown in Figure 2a, the jet can attach to either wall and will be stable in either position as long as symmetry exists. The unit is thus bistable. Warren(1) discusses the phenomena in more detail.

By introducing flow from a control jet, as shown in Figure 2b, the original jet can be switched to the opposite wall. This is illustrated in Figure 2c. Warren and Peperone(2) point out that as long as the jet output stagnation pressure is greater than the control jet input stagnation pressure, the device may be referred to as a bistable fluid amplifier.

In the General Electric report(3), it explains that one of the features of the bistable fluid amplifier that sets it apart from its analogous electronic counterpart is the fluid amplifier's stable response to a control signal under various conditions of temperature

and dynamic loading. Whereas the electronic device shows wide
fluctuations in its behavior under different temperature and load
conditions, the response of the fluid device remains relatively
stable. The General Electric report(3) points out that bistable
fluid amplifiers have been subjected to environments up to 50g
with no apparent affect on the device. The same source states that
Bendix has tested other fluid amplifiers up to 1400°F with performance
generally as predicted. Madonna, Harris, and Anderson(4) also showed
that temperature had little affect on bistable fluid amplifier
switching. To exploit these stability characteristics, a rationale
should be utilized that establishes a physical geometry for the unit
itself. This requires a definition of stability.

The geometry that requires the largest change in control signal
for switching is the most stable. Stagnation pressure is that pressure
that would be obtained by bringing a moving fluid to rest isen-
tropically. In the Bernoulli Equation:

$$\rho \frac{V_2{}^2 - V_1{}^2}{2} + P_2 - P_1 + \rho g(Z_2 - Z_1) = 0$$

the stagnation pressure, henceforth referred to as pressure, can be
related to the energy of the fluid when the potential term involving
Z is not involved. The difference between the pressure in the control
jet without control flow and the pressure in the control jet with

the control flow necessary for switching is therefore a measure of
the kinetic energy of the control jet necessary for switching. This
change in control pressure necessary for switching can then be a
measure of the magnitude of the control signal necessary for switching.
A dimensionless parameter is obtained by taking the ratio of the
power jet pressure to the change in control pressure necessary for
switching. The geometric configuration that causes this parameter
to be a minimum is the most stable. Therefore, the parameter is
defined as the stability parameter.

By determining the stability parameter for different combinations
of wall angle, wall offset, and power jet pressure, a geometric
configuration is found that yields a minimum value of the stability
parameter. This configuration is the most stable.

Procedure

An existing wall attachment device with a single controller was used in the present investigation. McCoy(5) and Kirkpatrick(6) describe the construction of the device. A schematic of the unit is shown in Figure 3. The locations where the pressure and temperature measurements were made are also shown in this figure.

The power jet nozzle was milled from 6 X 12 X 2 inch aluminum blocks. The control jet nozzle was constructed from 1/2 X 2 inch steel stock. The walls were made from 2 X 2 X 26 inch hollow aluminum square stock. The bottom cover plate was 1/8 inch steel plate. The top cover plate was 3/16 inch aluminum plate to facilitate removal for changing the geometry. Joints were sealed with 1/8 inch porous rubber gasket. The gaskets were impregnated with a rubber cement to limit leakage. A non-hardening putty was used in some places to supplement the gaskets.

The power jet nozzle and control jet nozzle widths were held constant at 0.355 inch. Control jet stagnation pressure, P_{oc} , was measured with a wedge-head probe made by United Sensor and read on a 30 inch water manometer. Static pressure taps on each side of the wedge-head permitted the operator to keep the wedge-head aligned with the flow. Control jet static pressures at stations 1 and 2 were measured with wall taps and read on 30 inch water manometers. The static pressure tap at station 2, P_{sc2} , was disconnected midway through the tests to permit widening the unit. Power jet stagnation

pressure, P_{om} , was measured with a wedge-head probe and read on a 30 inch mercury manometer. Power jet static pressure, P_{sm} , at the power jet nozzle throat was measured with a wall tap and read on a 30 inch water manometer. Power jet stagnation temperature, T_o, was measured with a Century Thermometer using a mercury bulb placed in a well in the power jet stagnation chamber.

Air was supplied from a Schramm compressor rated at 200 scfm at 100 psi. Both power jet and control jet pressures were controlled with globe needle point valves. All tests were performed at power jet pressures in the range from 0.7 to 4.0 inches of mercury gauge.

With the control jet needle valve closed, the power jet pressure was brought to the desired value using the power jet needle valve. The pressure in the control jet nozzle, P_{oc} , was then noted. The control jet needle valve was then opened to permit air to bleed in and switch the unit. The pressure in the control jet nozzle at the instant of switching was recorded. Power jet pressure was held constant throughout the switching procedure. The test was repeated at six different power jet pressures. Thus, the unit was switched at six different power jet stagnation pressures for each geometric configuration of the device.

The wall on the side with the controller had 39 pressure taps connected to a water manometer board. The maximum, minimum, and ambient pressures and their locations along the wall were noted without control jet flow and again noted with control jet flow introduced.

Small strips of cloth were attached to the exhaust of the unit to facilitate determining to which wall the jet was attached and when switching occured. These strips were small enough that they did not constitute a load on the device.

The power jet stagnation pressure was corrected to standard sea level by using the following relationship:

$$P_{omg} - (29.92 - P_{atm}) = P_{om}$$

where all pressures are in inches of mercury and 29.92 is the standard atmospheric pressure at sea level in inches of mercury.

Results

The change in control pressure necessary to switch the unit is graphed versus power jet stagnation pressure for various geometries in Figure 4 through 10. It appears that a linear relationship exists between the change in control pressure necessary for switching and the power jet pressure. However, the slope or rate of change of this linear relationship differs for each geometry. Plots of this rate of change of ΔP_{oc} with P_{om} versus a geometric parameter are shown in Figures 11 and 12.

The stability parameter plotted against power jet pressure is shown in Figure 13. Three representative geometric configurations were chosen to show that the stability parameter does not vary widely with power jet pressure.

In Figures 14 through 17, the stability parameter is shown plotted against wall angle for different conditions of wall offset and power jet pressure. Each of these four figures is at a different power jet pressure. The four graphs in each figure are at four different wall offsets.

Discussion

The pressure gain of a bistable fluid amplifier is defined as
the ratio of the output stagnation pressure to the control stagnation
pressure necessary to switch the unit. Kirshner(7) implied that the
results of increasing the wall offset, δ, or the wall angle, α,
would have similar effects on the gain of the amplifier. Beeken(8),
Katz(9), and a number of other sources have been found that show
the effect on gain of varying the unit geometry. Increasing the
wall offset decreases the gain up to an offset of about two nozzle
widths, then increases the gain. Increasing the wall angle increases
the gain for small wall angles.

That the geometry resulting in the maximum gain would not be the
same as the geometry resulting in the minimum stability parameter
is a valid assumption. However, as long as the unit demonstrates
the basic property of an amplifier, the output stagnation pressure
being greater than the control input pressure, the magnitude of the
gain is of little concern in this study.

Examining the stability parameter from the aspect of power jet
pressure, there is little variance in the stability parameter at
different power jet pressures as long as the geometry is the same.
This is shown in Figure 13. It can also be seen by examining Figures
14 through 17.

Now, looking at the stability parameter with respect to the
wall angle, there is a definite minimum value for the stability

parameter. Looking at Figures 14 through 17, the minimum value occurs at a wall angle of 20° for a wall offset of 0.5 inch; 30° for a wall offset of 1.0 inch; returning to 20° for a wall offset of 2.0 inches; and to 18° for a wall offset of 3.0 inches. From this, the conclusion can be drawn that the minimum stability parameter occurs at a wall angle less than or equal to 30°.

The most stable configuration is found by examining the problem from the aspect of wall offset and wall angle combined. Figure 14 shows the parameter minimum to be 4.2 for an offset of 0.5 inch. The same figure shows the parameter has dropped to 2.4 for an offset of 1.0 inch. With a wall offset of 2.0 inches, the parameter has increased to 3.2 at its minimum value. For an offset of 3.0 inches in the same figure, the minimum value of the parameter has again dropped to 2.7. This downward trend should continue until the device is no longer bistable, and it takes on the characteristics of a proportional amplifier. This is concluded from examining the 20° curve in Figure 12. With increasing wall offset, the first maximum value of the change in control pressure necessary for switching occurs at an offset of 1.0 inch. A wall offset of 1.0 inch for the device tested is 2.8 nozzle widths. McCoy(5) predicted that a wall offset between two and four nozzle widths would result in the most strongly attached jet. The 1.0 inch offset lies in this range, thus substantiating his results. Examining the 1.0 inch wall offset curves in Figures 14 through 17, shows the stability parameter reaches a minimum value at 30° in all four figures. Therefore, the most stable

geometric configuration of the device using the rationale of the stability parameter is wall angle at 30° and wall offset at 1.0 inch.

Using the wall pressure distribution data to locate the maximum pressure location and assuming that point to be the termination of the attaching streamline was the basis for a different approach to the stability problem. The attaching streamline was drawn on a schematic of the unit under conditions of control flow introduced and of no control flow. The volume of the recirculation bubble encompassed by the streamline and the unit's walls was then determined with the aid of a planimeter. The change in the bubble's volume from a condition of no control flow to a condition of the control flow required for switching to occur was determined for different unit geometries. However, no geometric configuration resulted in maximizing or minimizing the change in control volume necessary for switching.

Since switching the attached jet to the opposite wall entails adding energy to the unit, a thermodynamic approach to the stability problem was attempted. This approach required the utilization of the change in control pressure necessary for switching and the change in bubble volume necessary for switching. However, since there was simultaneous changes in both mass being introduced and volume encompassed, neither a control mass nor a control volume analysis could be accomplished.

Using a dimensionless parameter similar to the stability parameter defined here, Beeken(5) did an experimental study of a curved wall

device as opposed to a straight wall device. His results were different when he varied the offset. On a plot similar to those in Figures 14 through 17, he had a minimum point at 0.8 nozzle width. This corresponds to a 0.3 inch wall offset with the straight wall equipment. The reason for the difference between the minimum point occuring at 0.8 nozzle width with the curved wall device instead of 2.8 nozzle widths with the straight wall device is the fact that a curved wall significantly reduces the size of the recirculation bubble. With the straight wall device, as the wall offset increases, the volume of the bubble also increases. This requires a larger control flow to cause the bubble to slide down the wall and switch the attached jet.

In defense of the straight wall device, a curved wall unit would be extremely difficult to analyze. If the stability and gain of a straight wall device were similar to the stability and gain of a curved wall unit, the former would be easier and less expensive to fabricate.

As an aside, a rather unscientific test was performed. To see how this particular unit reacted to dynamic loading, the control jet was introduced to a point just below that necessary for switching to occur. The entire assemble, table and all, was lifted a few inches off the floor and dropped. No switching occured.

Bibliography

1. Warren, R. W., Wall Effect and Binary Devices, Proceedings of the
   Fluid Amplification Symposium, Volume I, Diamond Ordnance Fuze
   Lab, Washington, D.C., October 1962.

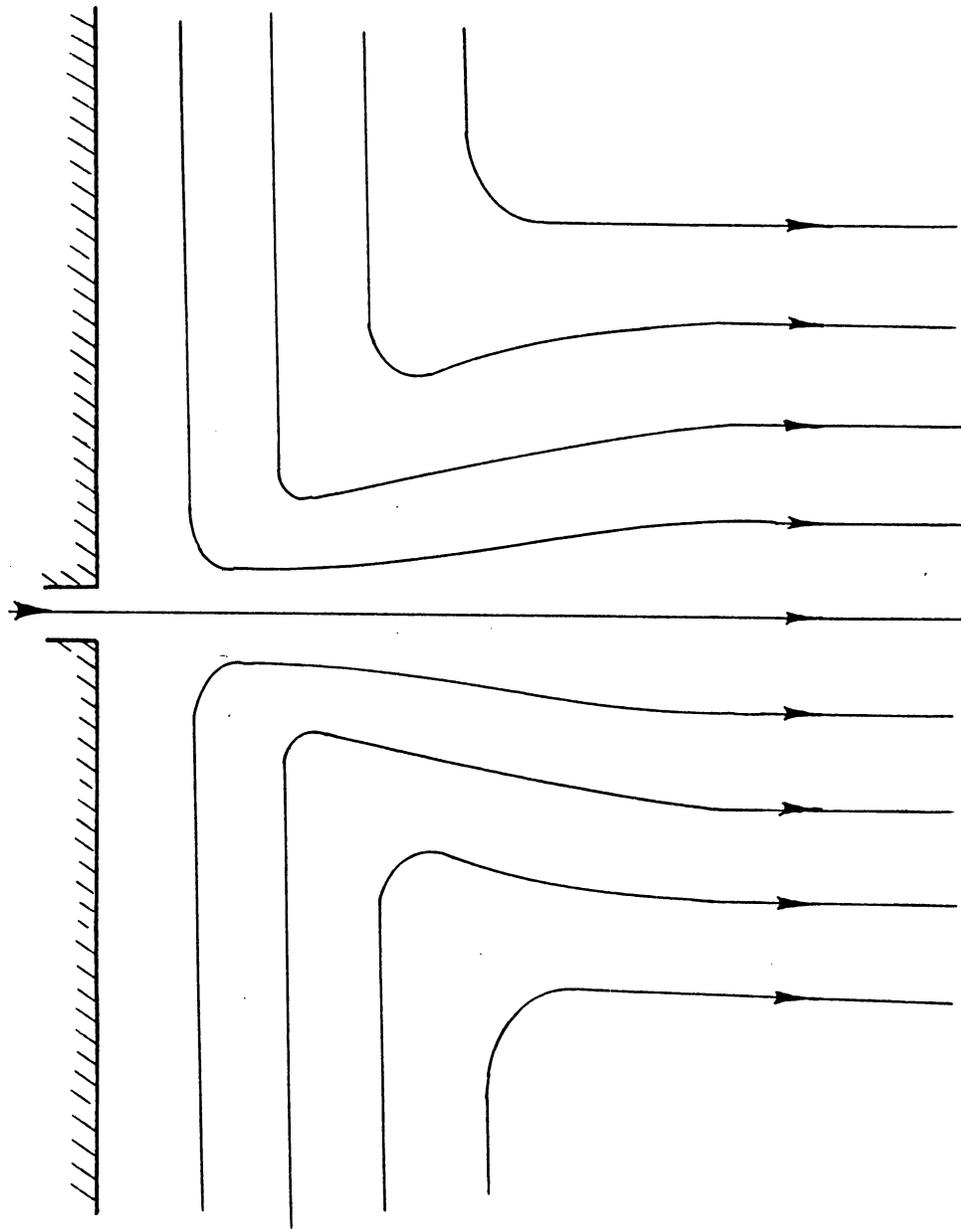2. Warren, R. W., Peperone, S. J., Fluid Amplification, 1. Basic
   Principles, Diamond Ordance Fuze Lab, Department of the Army,
   Washington, D.C., August 1962.

3. General Electric Company, Fluid Amplifier State of the Art,
   Volume I, Research and Development-Fluid Amplifiers and
   Logic, Schenectady, New York, 1964.

4. Madonna, M. A., Harris, W. J., Anderson, R. C., Investigation
   of the Environmental Effects on Pure Fluid Amplifiers,
   American Society of Mechanical Engineers, New York, December 1968.

5. McCoy, J. J., Jr, An Experimental Study of the Effect of the
   Aspect Ratio, Wall Angle, and Wall Offset on the Resultant Force
   on the Two-Dimensional Jet in Bistable Fluid Amplifiers, Thesis
   submitted at Rice University, September 1967.

6. Kirkpatrick, J., An Experimental Study of the Pressure Contours
   in the Turbulant Reattachment Bubble of a Bistable Fluid
   Amplifier, Thesis submitted at Rice University, January 1968.

7. Kirshner, J. M., Fluid Amplifiers, First Edition, McGraw-Hill,
   1966.

8. Beeken, B. B., _A Theoretical and Experimental Study of a Coanda Curved Wall Attachment Device_, American Society of Mechanical Engineers, New York, December 1968.

9. Katz, S., _An Introduction To Proportional Fluid Control_, Proceedings of the Fluid Amplification Symposium, Volume I, Diamond Ordance Fuze Lab, Washington, D.C., October 1962.
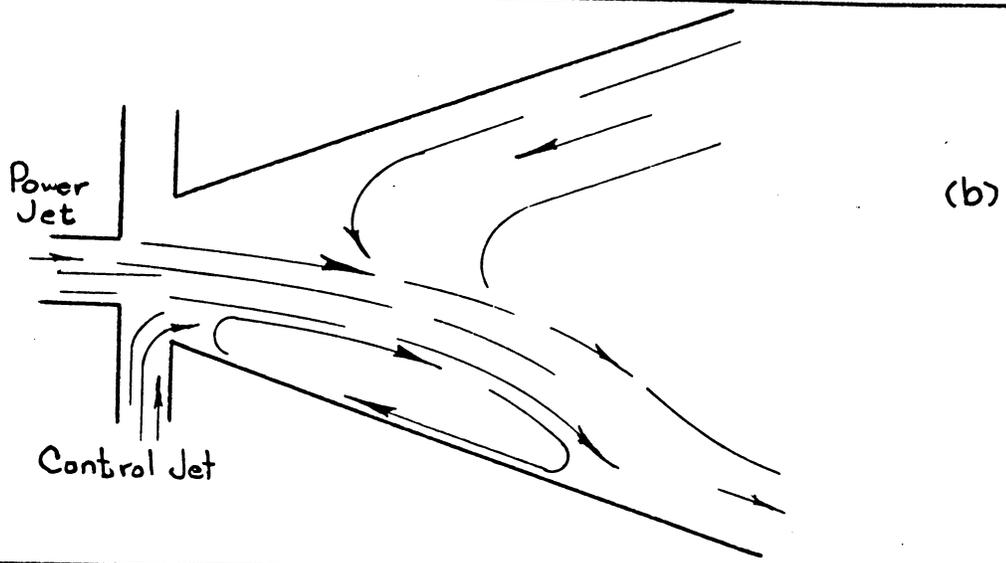
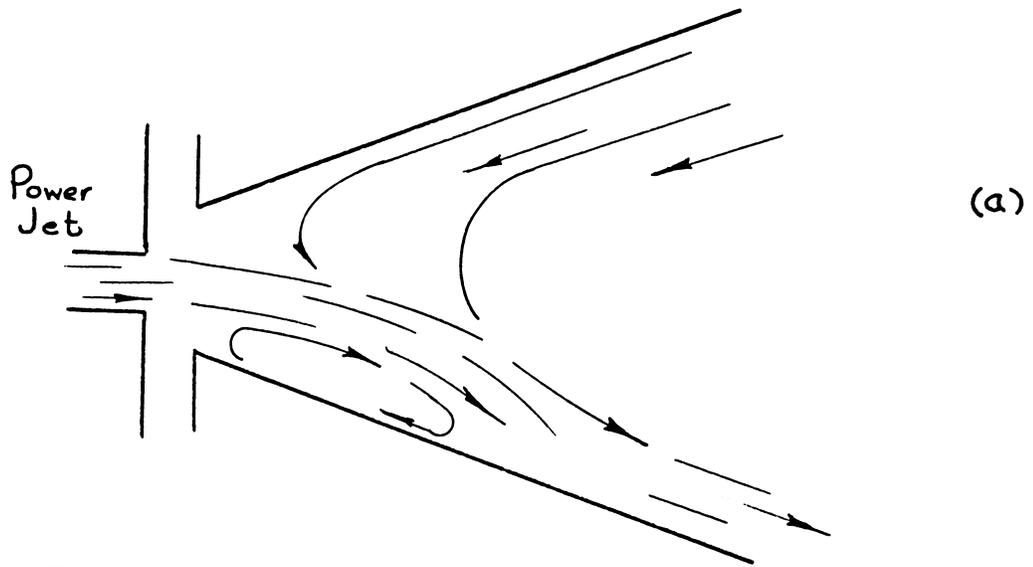FIG. 1 - Free Jet Showing Entrainment Of Ambient Fluid

Power
Jet

(a)

Power
Jet

Control Jet

(b)

Power
Jet

Control Jet

(c)
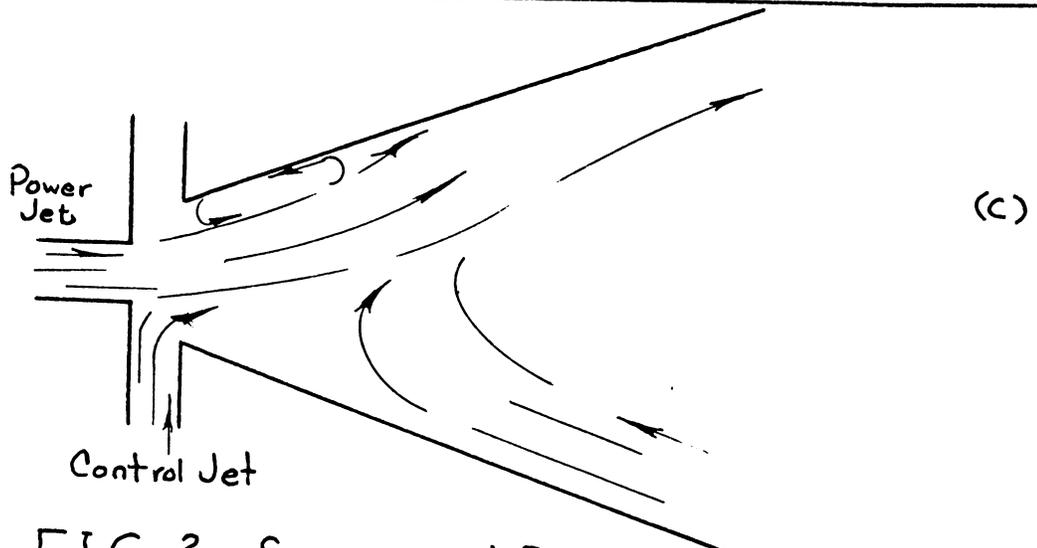
FIG. 2 - Switching A Bistable Fluid Amplifier
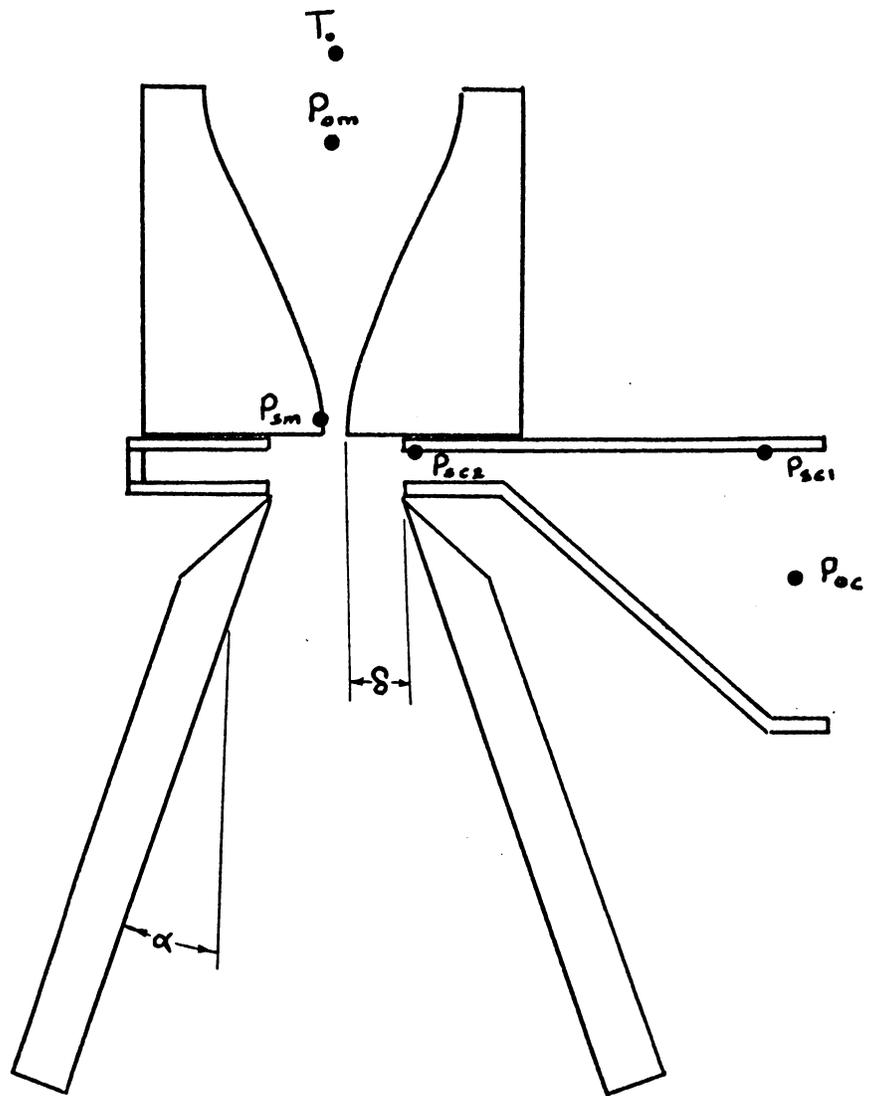
FIG. 3

Fluid Amplifier Schematic
Showing Pressure & Temperature
Measurement Locations.

FIG. 4

Offset ... 0.5 inch
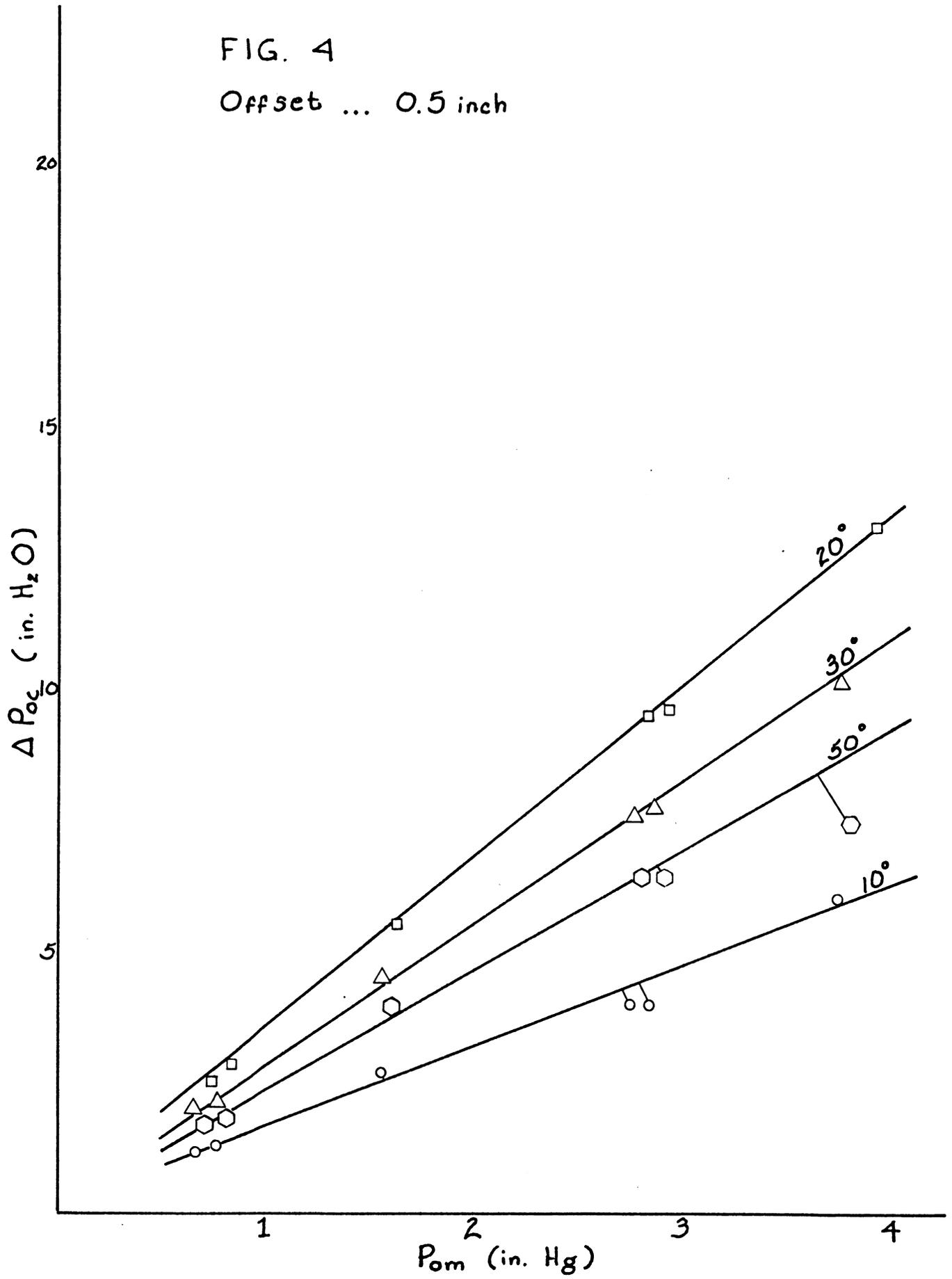
FIG. 5

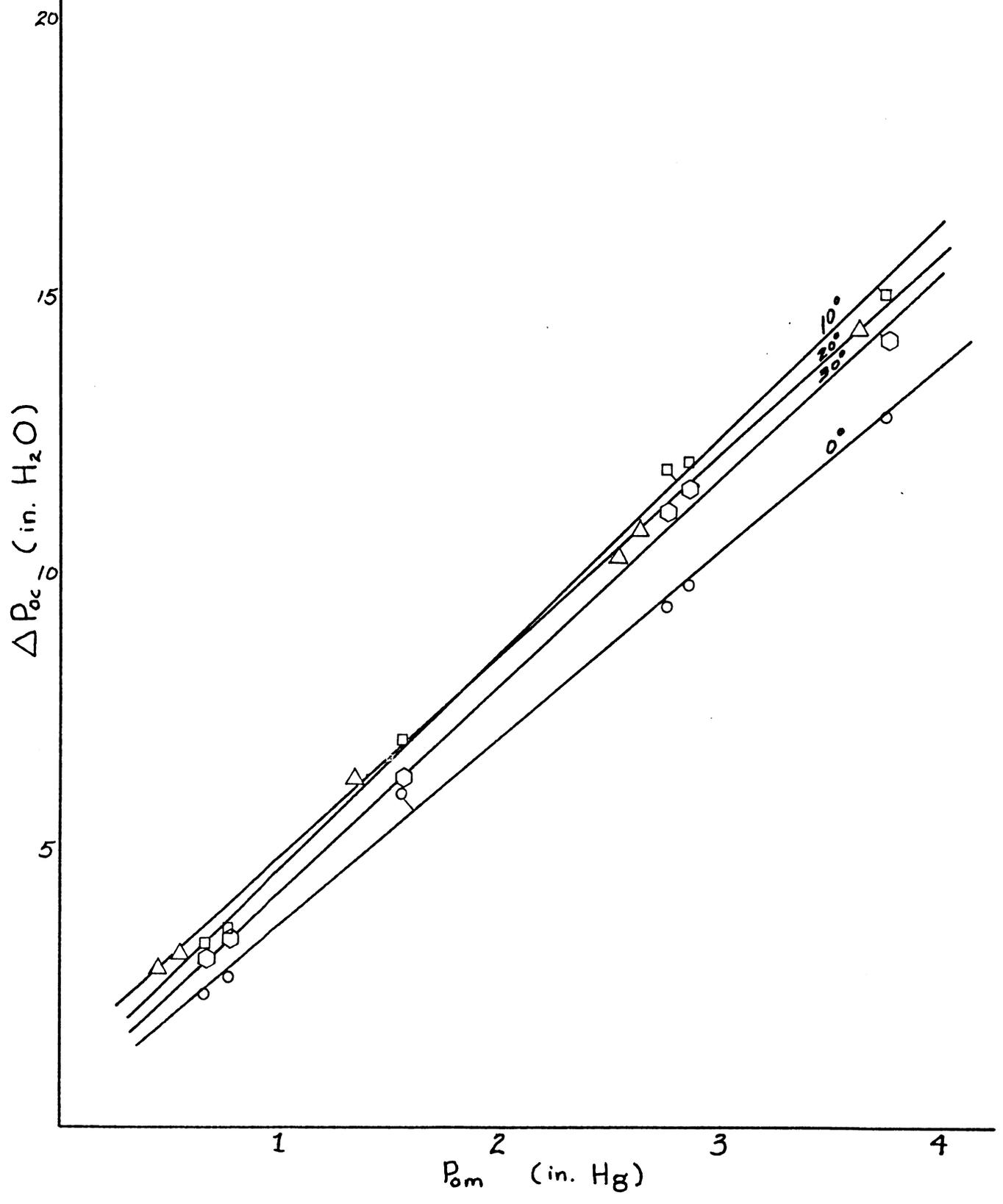Offset ... 1 inch
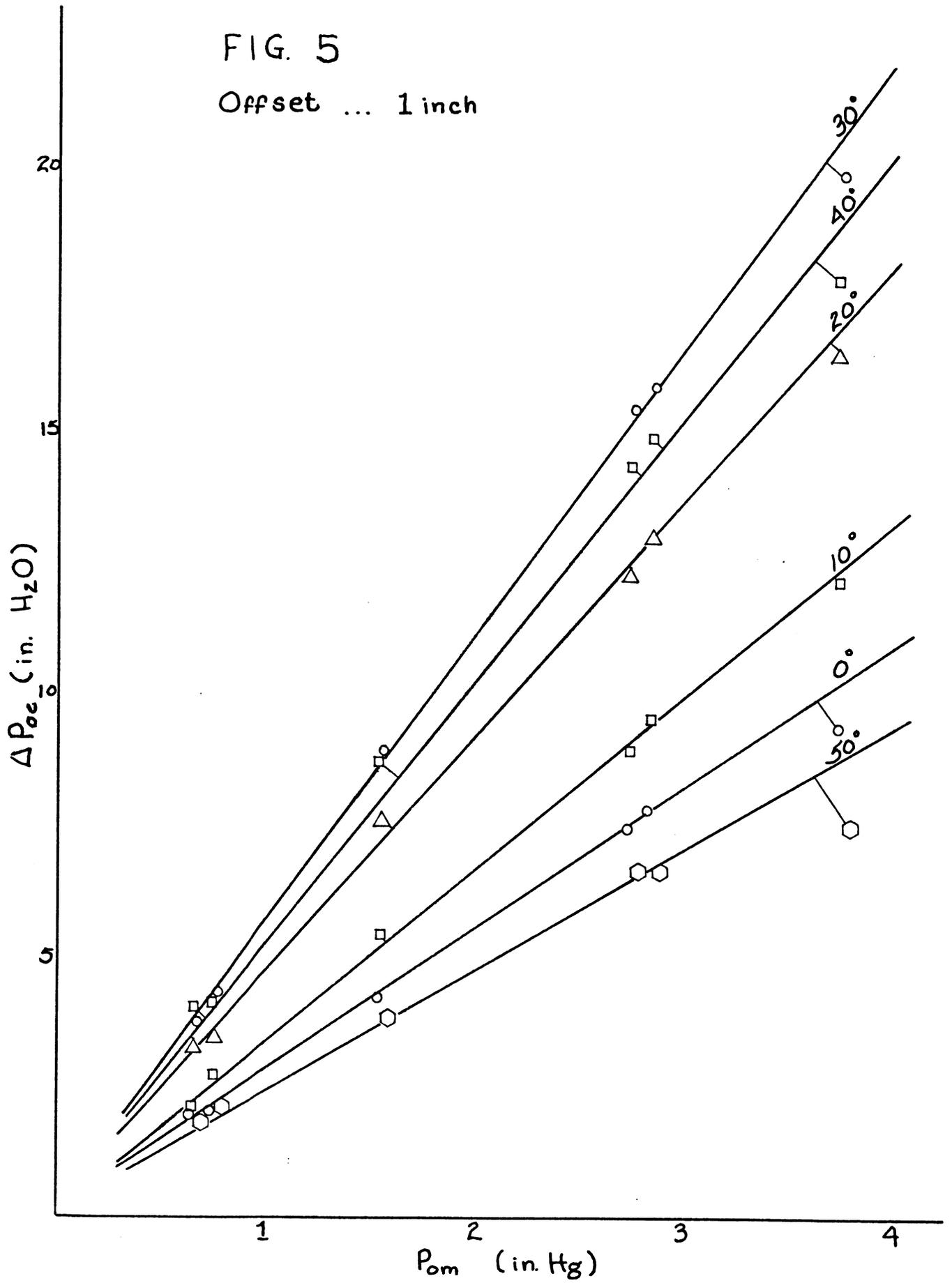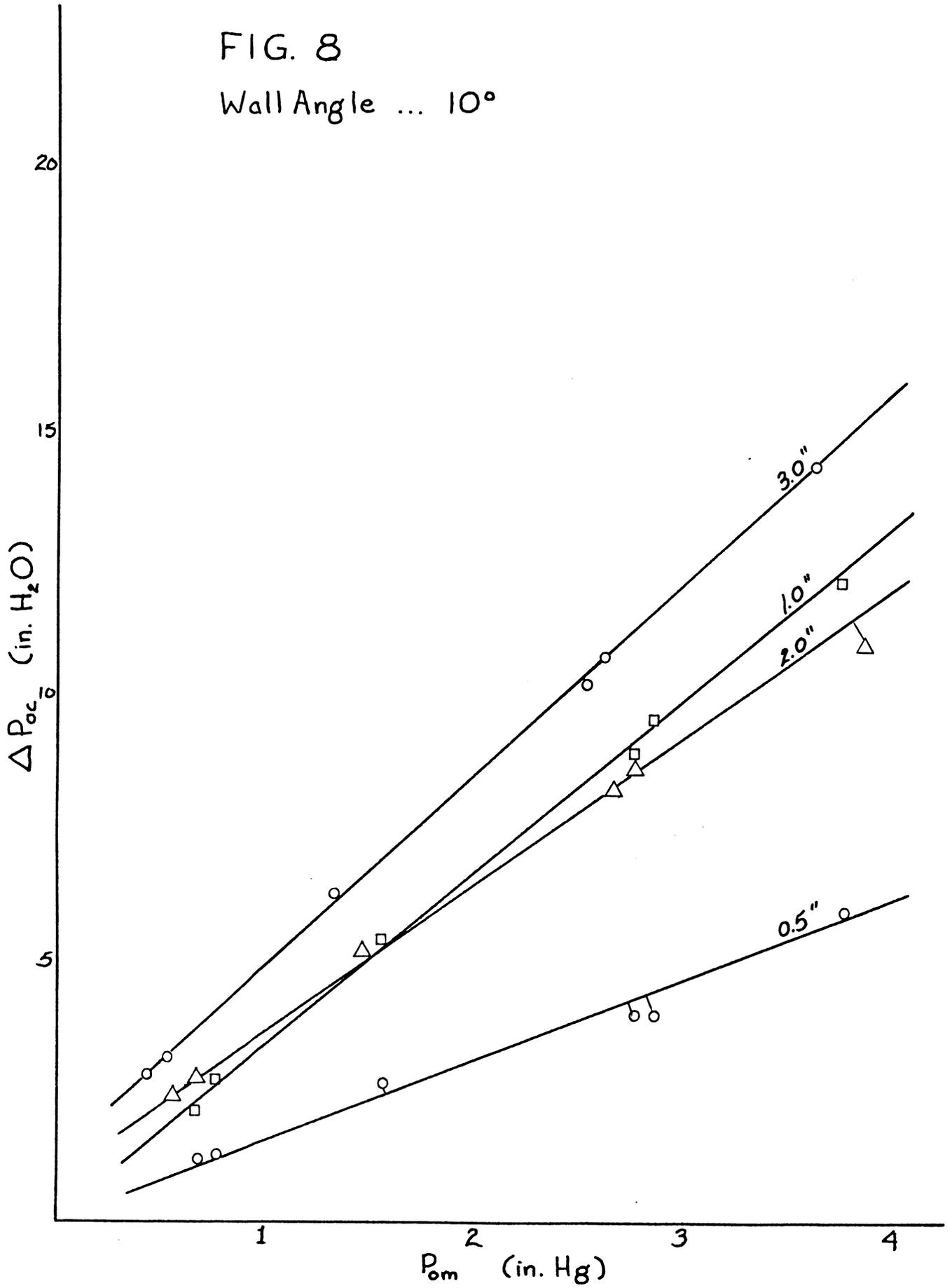
FIG. 6

Offset ...2 inch
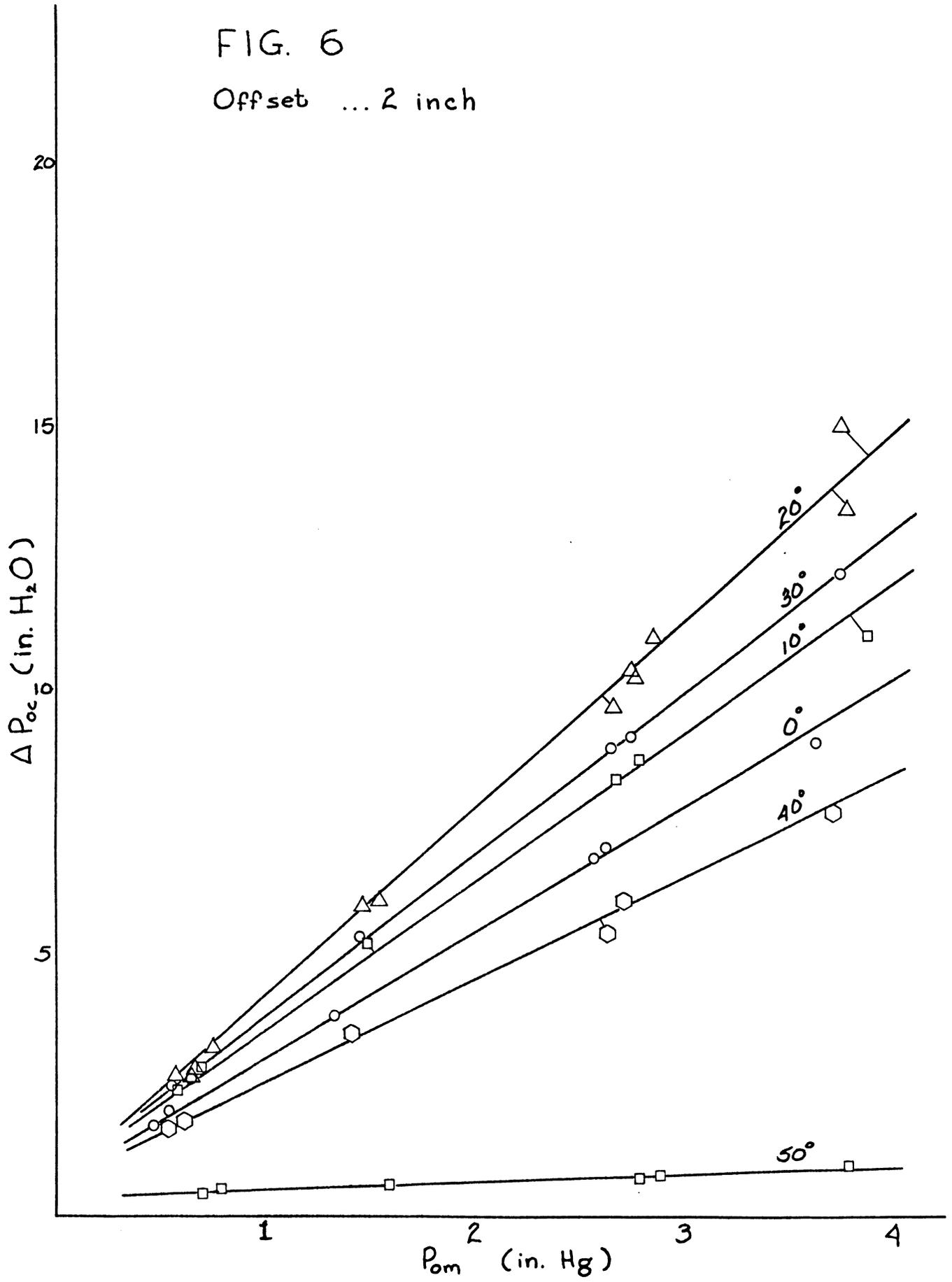
FIG. 7
Offset ... 3 inch

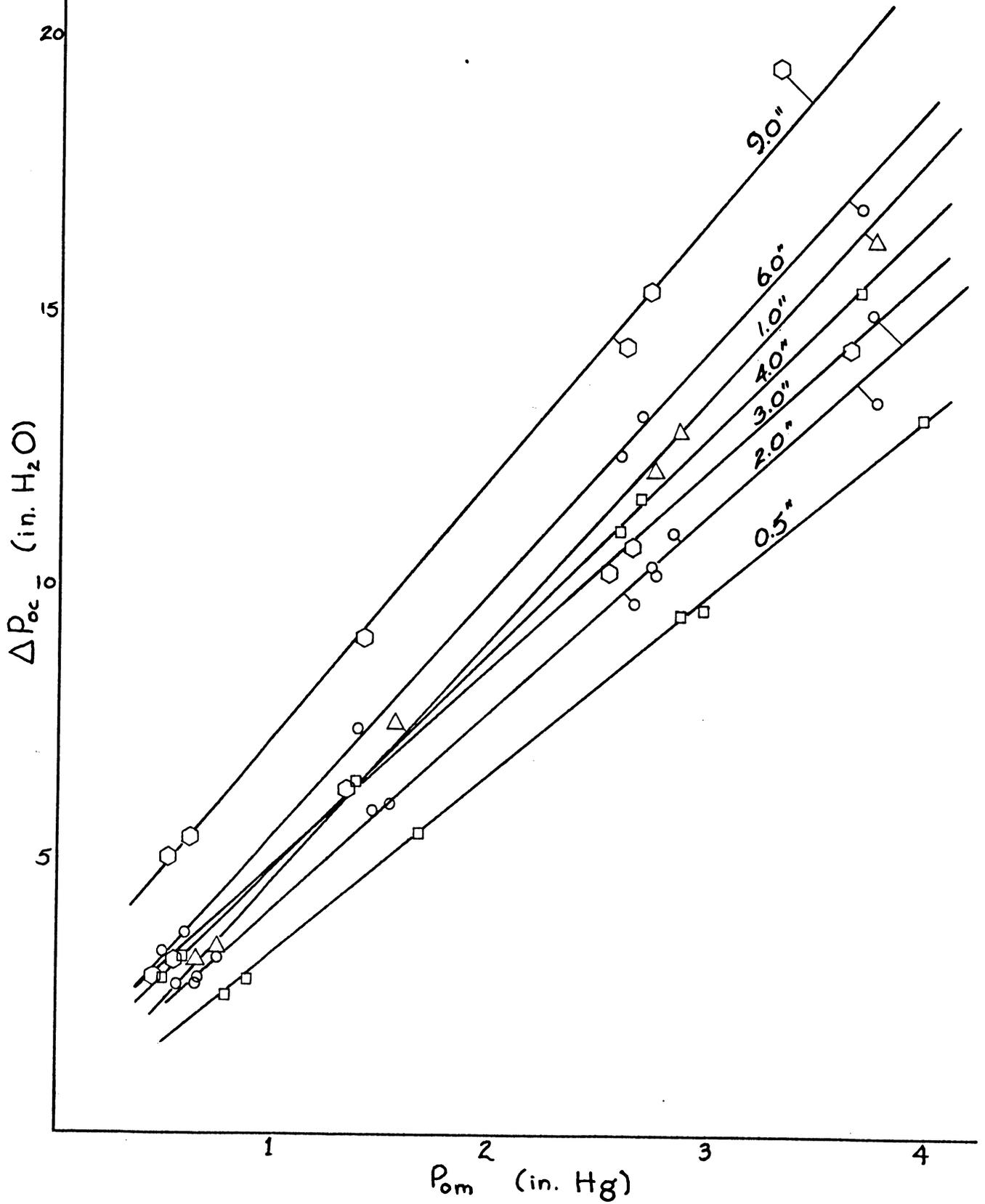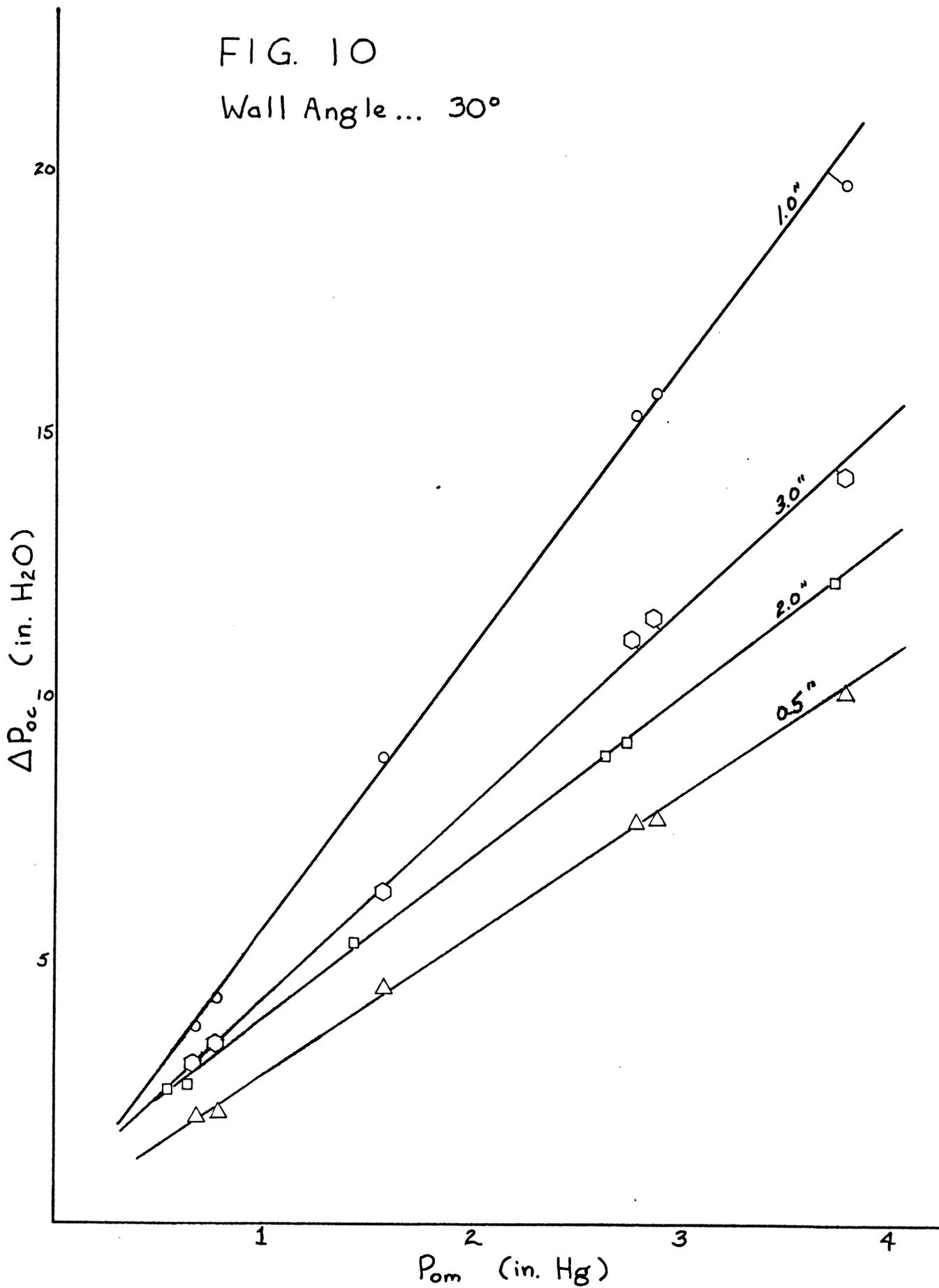FIG. 8

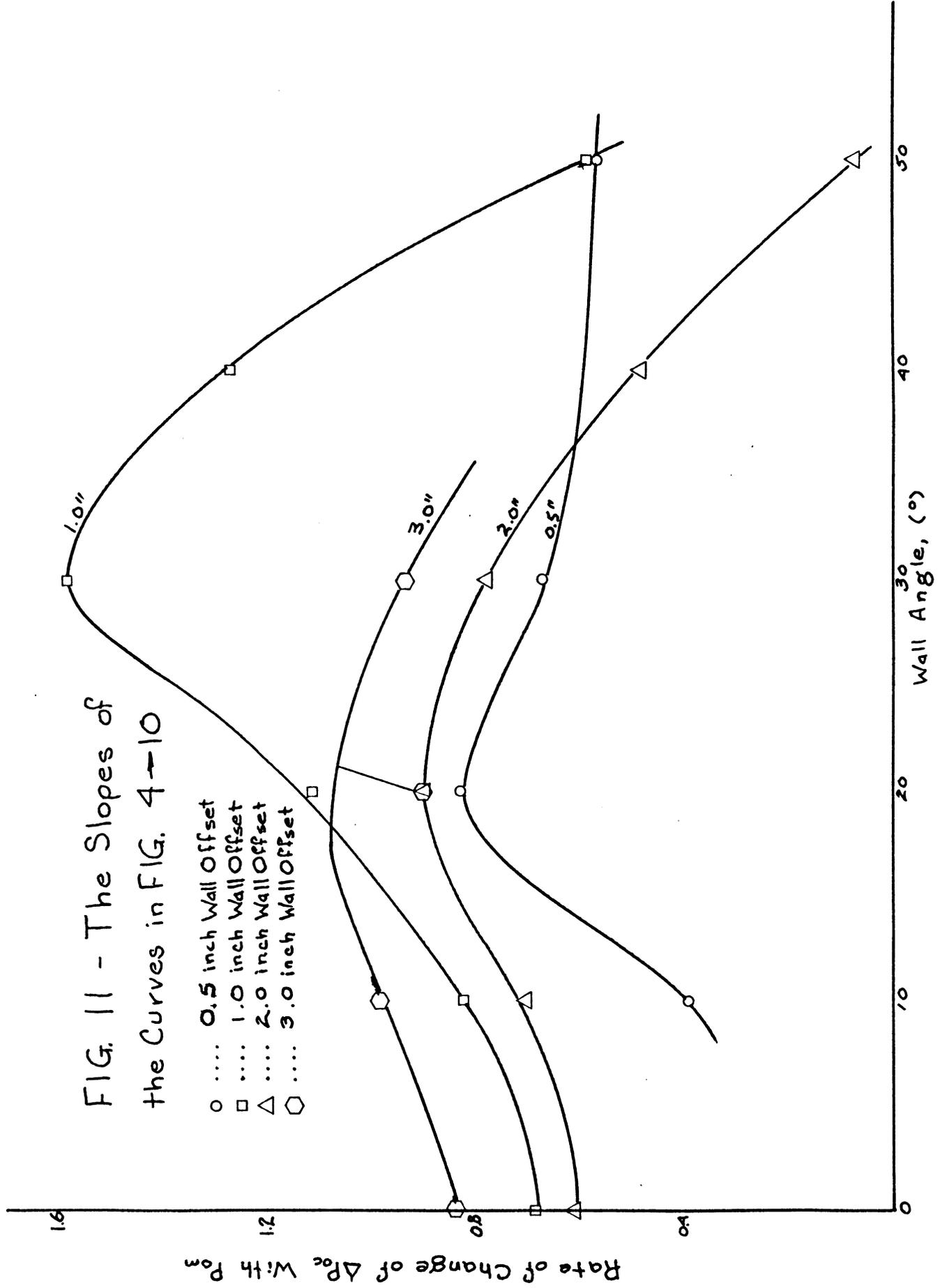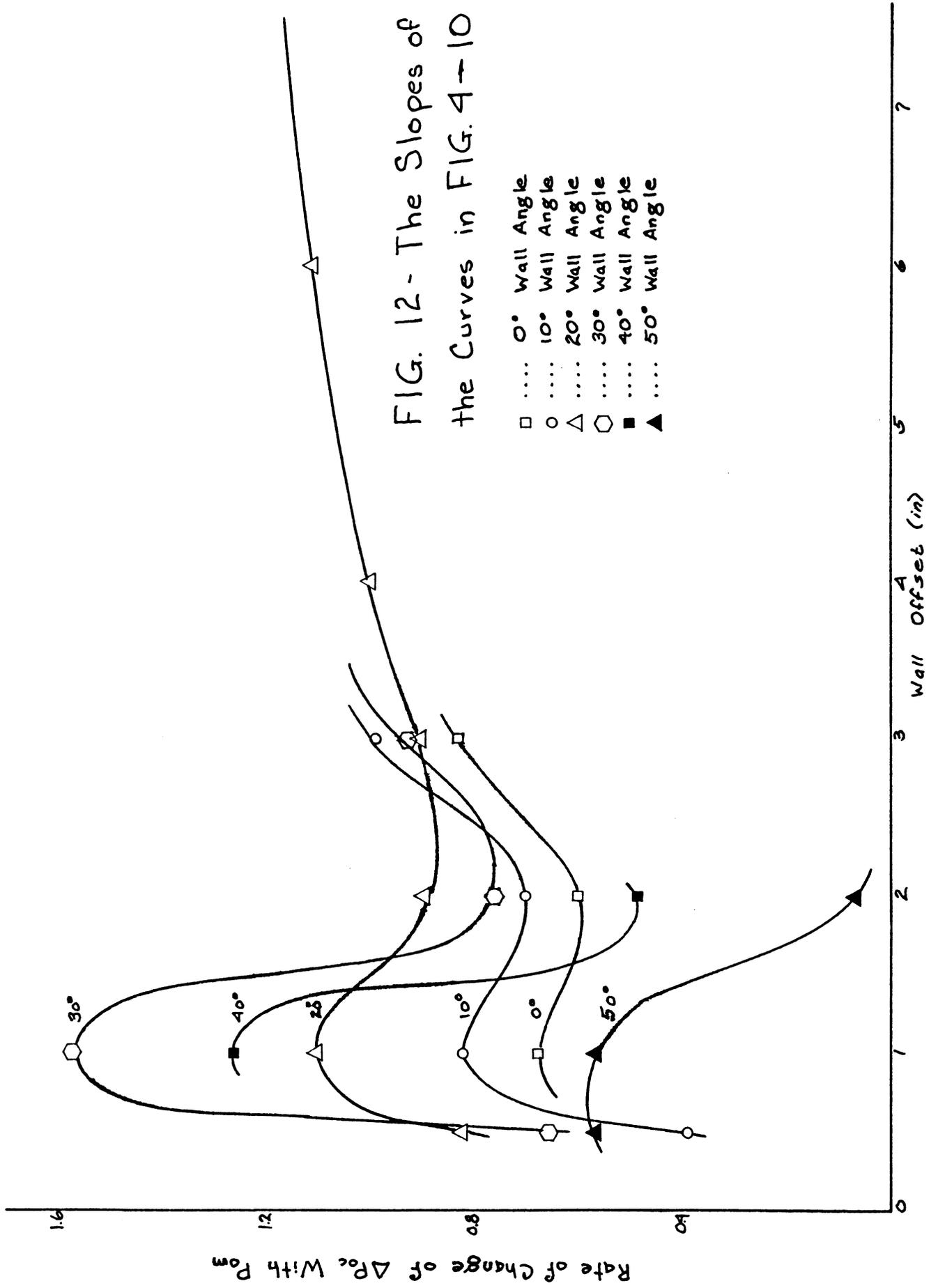Wall Angle ... 10°

FIG. 9
Wall Angle ... 20°

FIG. 10
Wall Angle ... 30°

FIG. 11 – The Slopes of the Curves in FIG. 4→10

o .... 0.5 inch Wall Offset
□ .... 1.0 inch Wall Offset
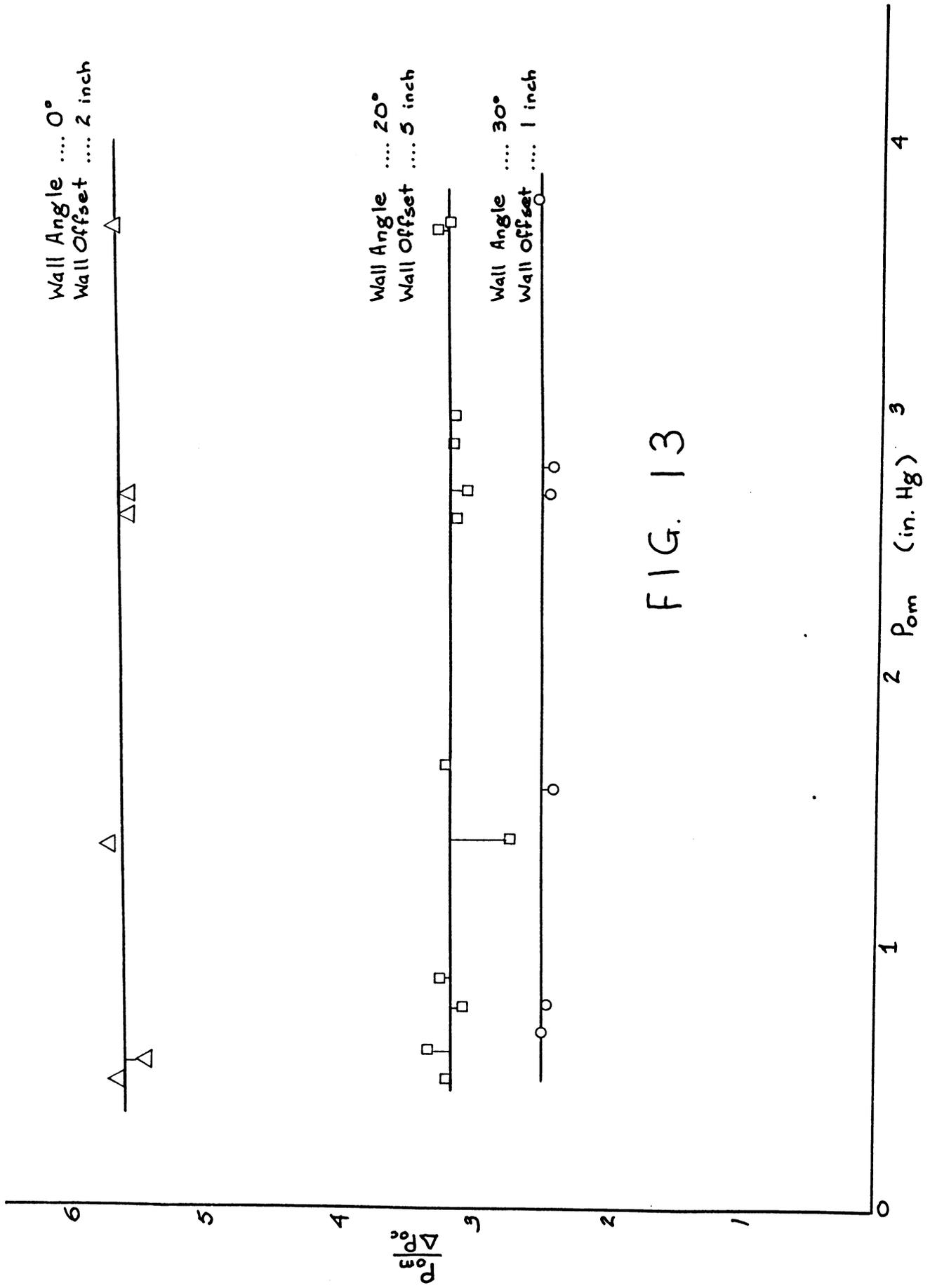△ .... 2.0 inch Wall Offset
⬠ .... 3.0 inch Wall Offset

Rate of Change of ΔP_{oc} With P_{om}

Wall Angle, (°)

FIG. 12 - The Slopes of
the Curves in FIG. 9-10

□ ···· : 0° Wall Angle
○ ···· : 10° Wall Angle
△ ···· : 20° Wall Angle
⬠ ···· : 30° Wall Angle
■ ···· : 40° Wall Angle
▲ ···· : 50° Wall Angle

Wall Offset (in)

Rate of Change of ΔP$_{oc}$ With P$_{om}$

Wall Angle .... 0°
Wall Offset .... 2 inch

Wall Angle .... 20°
Wall Offset .... 5 inch

Wall Angle .... 30°
Wall Offset .... 1 inch

$\dfrac{\Delta P_{om}}{P_{oc}}$

P_{om} (in. Hg)

FIG. 13

FIG. 14

o .... 0.5 in. Wall Offset
□ .... 1.0 in. Wall Offset
△ .... 2.0 in. Wall Offset
⬠ .... 3.0 in. Wall Offset

P_{om} .... 1.0 in. Hg

FIG. 15

o .... 0.5 in. Wall Offset
□ .... 1.0 in. Wall Offset
△ .... 2.0 in. Wall Offset
⬠ .... 3.0 in. Wall Offset

P_{om} .... 2.0 in. Hg

FIG. 16

o .... 0.5 in. Wall Offset
□ .... 1.0 in. Wall Offset
△ .... 2.0 in. Wall Offset
⬠ .... 3.0 in. Wall Offset

P_{om} .... 3.0 in. Hg

FIG. 17

o .... 0.5 in. Wall Offset
□ .... 1.0 in. Wall Offset
△ .... 2.0 in. Wall Offset
⬠ .... 3.0 in. Wall Offset

P_{om} .... 4.0 in. Hg

Wall Angle, (°)

$\frac{P_{om}}{\Delta P_{oc}}$